INVESTIGATION OF DORSAL FIN EFFECTS ON THE AERODYNAMIC PERFORMANCE OF INVERTED-V EMPENNAGE VTOL UNMANNED AERIAL VEHICLE

Muhammad Agung Bramantya [1], Gesang Nugroho [2]

[1] Department of Mechanical and Industrial Engineering, Faculty of Engineering

Gadjah Mada University

Jl. Grafika No. 2 Kampus UGM Yogyakarta 55281 Daerah Istimewa Yogyakarta, Indonesia

bramantya@ugm.ac.id [1]

Abstract

Unmanned Aerial Vehicles (UAVs) are essential tools in precision agriculture, enabling real-time monitoring, improved land management, and more efficient resource use. Among them, Vertical Takeoff and Landing (VTOL) UAVs are ideal for operation in confined and uneven agricultural terrains. However, UAVs equipped with inverted-V empennages suffer from aerodynamic drawbacks including directional instability and adverse yaw under sideslip conditions. This study advances the state-of-the-art by optimizing the aerodynamic performance of inverted-V tail configurations through integration of a dorsal fin. Using Computational Fluid Dynamics (CFD), we assessed multiple dorsal fin designs on a UAV platform with a maximum takeoff weight of 10 kg, payload of 2 kg payload, 2-hour endurance, stall speed of 10 m/s, and operational range of 5 km². We analyzed key aerodynamic metrics—lift and drag coefficients, lift-to-drag ratio, and yaw moment coefficient—as well as flow behavior via pressure contours and vorticity plots. The results confirmed that sideslip angles degrade aerodynamic efficiency; however, a properly designed dorsal fin, particularly variation 2, significantly reduced adverse yaw at higher angles of attack and sideslip. This modification enhances UAV stability and flight performance, indicating a meaningful improvement in VTOL UAV design for agricultural applications.

Key words : aerodynamic, unmanned aerial vehicles, CFD, dorsal fin.

INTRODUCTION

Unmanned Aerial Vehicles (UAVs) have undergone significant technological advancements in recent years, positioning them as invaluable tools across various industries, particularly precision agriculture [1]. Precision agriculture refers to the integration of advanced technologies such as UAVs to optimize farming practices, improve productivity, and reduce resource consumption [2]. UAVs have become central to modern agricultural practices owing to their capacity to provide real-time, high-resolution data. They enable farmers to monitor crop health, soil conditions, and overall field performance, facilitating data-driven decisions that enhance land management and operational efficiency [3]. UAVs offer substantial advantages over traditional methods, significantly reducing the time and labor required for field surveys, and enhancing the accuracy of the data collected. This capability is essential for both small- and large-scale agricultural operations, as it allows for more efficient resource management while optimizing crop yield and reducing environmental impacts [4].

Among the various UAV configurations, vertical takeoff and landing (VTOL) UAVs have emerged as particularly well suited for agricultural applications. VTOL UAVs can take off and land vertically, eliminating the need for long runways, making them ideal for deployment in rural and agricultural environments where the space for conventional takeoff and landing is limited [5]. The compact nature of VTOL UAVs also allows for easy transport and deployment, which is particularly advantageous in remote or difficult-to-reach areas where infrastructure may be inadequate. Despite these advantages, optimizing the performance of VTOL UAVs in demanding agricultural environments presents several challenges, particularly regarding the aerodynamic efficiency of the empennage configuration.

A common empennage configuration used in VTOL UAVs is an inverted-V design that provides stability and maneuverability during flight [6]. However, this configuration is not without its aerodynamic challenges. In particular, inverted-V empennage can experience aerodynamic instability, particularly at higher sideslip angles, which occur frequently during turns or in the presence of crosswinds [7]. These instability issues lead to adverse yaw moments, which can degrade the

control and stability of UAV, making it particularly difficult to maintain a steady flight during surveillance or data collection tasks in turbulent or gusty wind conditions [8].

To address these aerodynamic challenges, this study explored the integration of a dorsal fin into an inverted V-shaped empennage configuration. The dorsal fin serves as an additional aerodynamic surface that enhances the stability of the UAV by reducing the adverse effects of sideslip angle and yaw moment [9]. Previous research has demonstrated that such modifications can improve the control of a UAV over its aerodynamic characteristics, particularly in the domains of lateral and directional stability, where yaw instability is the most problematic [10]. By increasing the effectiveness of the empennage, the dorsal fin improves the overall UAV performance, making it more suitable for precision agriculture missions.

The methodology employed in this study relies heavily on Computational Fluid Dynamics (CFD) simulations, which allow for detailed evaluation of various dorsal fin configurations and their impact on UAV performance. These simulations analyzed key aerodynamic parameters, including the lift and drag coefficients, lift-to-drag ratios, and yaw moments, under varying operational conditions [11]. Furthermore, this study investigated the airflow patterns within the UAV system, including the pressure contours and vorticity, to gain a deeper understanding of how the dorsal fin influences the overall aerodynamic behavior of the UAV.

The primary objective of this study was to enhance the performance of VTOL UAVs, particularly for precision agriculture applications, by optimizing the empennage design. By exploring various dorsal fin configurations, this study aimed to improve the lateral stability of VTOL UAVs, thus making them more reliable and efficient in agricultural settings [12]. The results of this study are expected to contribute significantly to the development of more stable UAV systems, further advancing UAV technology in precision agriculture. Ultimately, the findings of this study could support the broader adoption of UAV systems in agricultural practices, contributing to the technological advancement and sustainable growth of agriculture in Indonesia and globally [13].

METHODS

This section describes the methodology used to design and optimize UAV for precision agricultural surveillance. This study primarily utilized Computational Fluid Dynamics (CFD) simulations to evaluate the aerodynamic performance of dorsal fins integrated with an inverted V-empennage configuration. The design process began with the overall UAV configuration, specifically tailored for surveillance in agricultural environments, to ensure suitability for the limited space and operational requirements that are typical of such missions. First, key design parameters, including the size, weight, payload capacity, and mission endurance of the UAV, were established. The next step involves incorporating dorsal fins to improve lateral stability and reduce yaw moments, which are critical for maintaining control under high-sideslip conditions. CFD simulations were conducted using various dorsal fin designs to analyze their impact on aerodynamic parameters such as lift, drag, and yaw moment coefficients. This iterative approach allows for the refinement of both UAV design and dorsal fin configurations for optimal performance in precision agriculture applications.

This study used various tools to support the design process, data collection, and data analysis. Several software applications are used in this study.

- Microsoft Excel was used to organize and process numerical data.
- Autodesk Inventor 2024: 3D modeling and design of UAV geometry.
- ANSYS Design Modeler: Creation and refinement of aerodynamic design.
- ANSYS Mesh: Used to generate the computational grids essential for CFD simulations.
- ANSYS Fluent: Simulates the fluid dynamics around the UAV and analyzes its aerodynamic behavior.

This study involved conducting computational fluid dynamics (CFD) simulations on dorsal fins with an inverted V-shaped empennage. 3D models of the dorsal fins were developed using the approach described in the Aerodynamic Design Guidelines of Aircraft Dorsal Fin [8]. The dimensions of the dorsal fins used in this study are summarized in Table 1, which outlines the key parameters, including the vertical tail height (h_v), vertical tail area (S_v), dorsal fin area (S_{df}), sweep angle (ϕ_v), dorsal fin sweep angle (ϕ_{df}), and other geometric ratios, such as l_{df}/h_{df}, S_{df}/S_v, and ϕ_v/ϕ_{df}.

These variations provide a comprehensive framework for analyzing the aerodynamic impact of different dorsal fin designs, thereby enabling the optimization of UAV performance.

The independent variables in this study were the dorsal fins, which were designed with four-

dimensional variations and included parameters such as the height, length, sweep angle, and surface area. The dependent variable in this study was empennage configuration, specifically an inverted-V design. The control variables in this study included the Angle of Attack (AoA), sideslip angle, mesh size, and quality and size of the fluid domain used in the CFD simulations.

The 3D geometry of the UAV and dorsal fin was created using Autodesk Inventor CAD software. Simplifications are applied to the UAV geometry to reduce complexity during the meshing process. Four dorsal fin variations were developed, based on the independent variables established in this study.

Figure 1 shows the initial 3D model of the UAV, and Figure 2 shows a simplified model for meshing purposes. Additionally, Figures 3 (a) through (d) illustrate the four dorsal fin variations.

Table 1 Summary of geometry dorsal fin comparison

Para meters	Comparisons				Unit
	Var. 1	Var. 2	Var. 3	Var. 4	
Empennage Vertical Heigh (h_v)	0,270	0,270	0,270	0,270	m
Dorsal Fin Height, h_{df}	0,218	0,436	0,301	0,316	m
Empennage Vertical Area (S_v)	0,298	0,298	0,298	0,298	m^2
Dorsal Fin Area (S_{df})	0,094	0,179	0,179	0,094	m^2
Empennage Vertical Angle (φ_v)	22,21	22,21	22,21	22,21	deg
Dorsal Fin Angle (φ_{df})	77,1	66,4	77,1	66,4	deg
Empennage Vertical Length ($l_{v\text{-}df}$)	0,038	0,072	0,038	0,072	m
Dorsal Fin Length (l_{df})	0,218	0,109	0,150	0,237	m
Empennage Vertical Root Chord ($C_{r,v}$)	0,300	0,300	0,300	0,300	m
Dorsal Fin Root Chord ($C_{r,df}$)	0,073	0,073	0,073	0,073	m
$l_{v\text{-}df}/l_{df}$	0,174	0,659	0,252	0,303	-
h_{df}/h_v	0,805	1,613	1,112	1,169	-
l_{df}/h_{df}	1	0,25	0,5	0,75	-
S_{df}/S_v	0,315	0,6	0,6	0,315	-
$l_{df}/C_{r,v}$	0,726	0,363	0,501	0,790	-
S_v/S_{df}	3,17	1,67	1,67	3,17	-
φ_v/φ_{df}	0,28	0,33	0,28	0,33	-

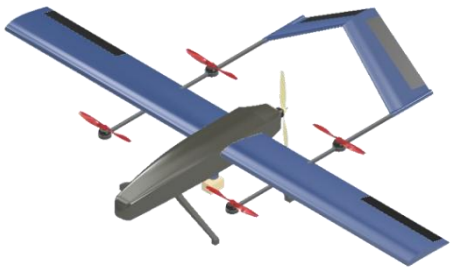

Figure 1 The initial 3D model of the UAV

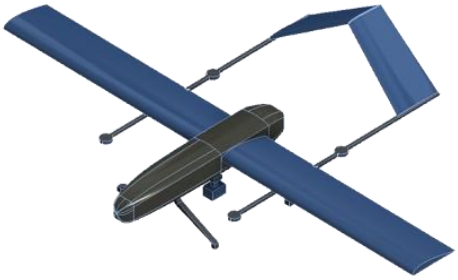

Figure 2 The simplified model for meshing purposes

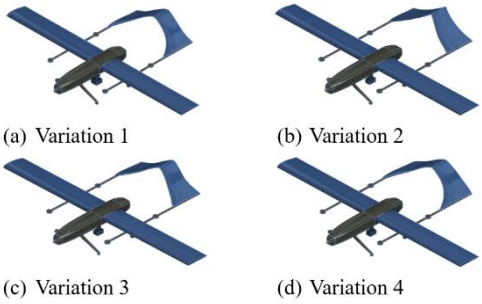

Figures 3 Four dorsal fin variations

RESULTS AND DISCUSSION

1. Impact of Dorsal Fin on Inverted-V Empennage

The aerodynamic effects of adding a dorsal fin were analyzed using Computational Fluid Dynamics (CFD) simulations, with a focus on lift, drag, and yaw moments derived from pressure contours and streamlines around the UAV. The pressure contours indicate that the pressure beneath the UAV was higher than that on its upper surface, indicating the generation of lift. As the angle of attack (AoA) increased, the lift also increased, accompanied by a higher drag, which reduced propulsion efficiency. Larger AoAs lead to airflow separation over the wings, potentially causing stall, a condition in which lift is lost at critical AoAs. Streamlines at low AoAs demonstrated a stable flow, whereas flow separation was observed at high AoAs.

Efficient UAV performance requires a balance between generating sufficient lift to maintain altitude and maneuverability, while minimizing drag. The L/D ratio (L/D) is a crucial performance indicator, as shown in Figure 4. At low AoAs (-9° to 5°), L/D remained stable across variations, suggesting a steady airflow around the wings and empennage. The maximum aerodynamic

efficiency was observed at AoAs between 9° and 12°, where the UAV generated high lift with minimal drag. Dorsal fin variation 1 achieved the highest L/D ratio at an AoA of 9°, exceeding 400, indicating an excellent aerodynamic efficiency. This variation effectively generated a significant lift with reduced drag. Figure 5 shows the airflow and vorticity for variations of 1.

At AoAs above 15°, the L/D ratios decreased for all variations owing to the increasing drag from the flow separation, which reduced the efficiency and led to stall. These results emphasize the importance of optimizing the dorsal fin design to improve the UAV aerodynamic performance, particularly in maintaining stability and efficiency under a high AoA.

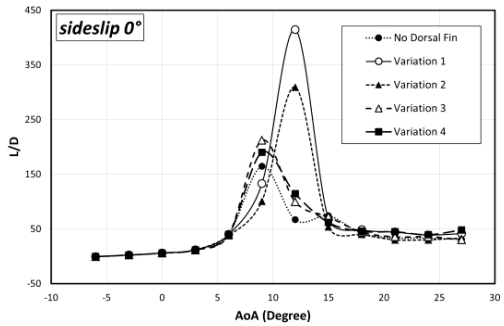

Figure 4 Graph of L/D vs AoA

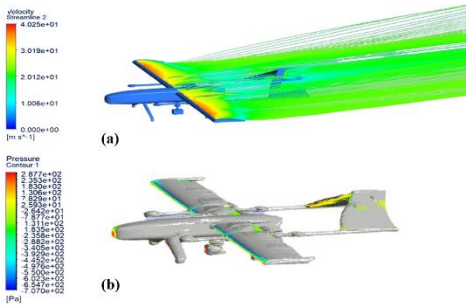

Figure 5 Phenomena in variation 1: (a) Airflow and (b) Vorticity

2. Analysis of the Effect of Sideslip Angle on the Dorsal Fin

This section provides a comprehensive analysis of the effects of sideslip angle on the aerodynamic performance and directional stability of a UAV equipped with an inverted V-shaped empennage. This study primarily examined several key aerodynamic parameters, including the coefficient of lift (C_L), coefficient of drag (C_D), lift-to-drag ratio (L/D), and coefficient of yawing moment (C_N), all of which are critical for assessing the flight efficiency, stability, and overall aerodynamic performance of UAVs.

The coefficient of lift (C_L) measures the ability of a UAV to generate lift at different angles of attack (AoA). At a sideslip angle of 0°, when the airflow was aligned with the UAV's longitudinal axis, the pressure distribution was optimal and facilitated the maximum lift generation. The results indicated that under these conditions, all dorsal fin variations produced similar C_L values, with the UAV exhibiting a relatively high lift coefficient across the range of AoAs tested.

However, as the sideslip angle increased to 5° and 10°, the presence of dorsal fins began to have a more pronounced impact on the lift of the UAV. Specifically, the results suggest that at these sideslip angles, the lift coefficient (C_L) decreases in certain AoA ranges, particularly between the 5° and 10° sideslip. This reduction in C_L can be attributed to the lateral wind components, which decrease the effective angle of attack, and consequently, the overall lift generation capability. The aerodynamic efficiency of the UAV was compromised under these conditions owing to the reduced lift produced by the dorsal fin.

Interestingly, the impact of the dorsal fins on lift became more noticeable at higher AoAs (18° to 27°), where the presence of dorsal fins tended to increase C_L compared with the baseline condition (i.e., no dorsal fin present). This improvement can be attributed to the ability of the dorsal fins to mitigate the adverse effects of turbulent flow and enhance pressure recovery over the wing, thereby enhancing the lift generation at a higher AoA. Therefore, while dorsal fins may reduce lift under certain low AoA and sideslip conditions, they provide a beneficial effect in maintaining lift at a higher AoA, particularly in high-sideslip flight regimes.

The coefficient of drag (C_D) is a vital parameter for evaluating the resistance encountered by UAV during flight. A higher drag coefficient indicates increased resistance, which typically results in a reduced aerodynamic efficiency and higher fuel consumption. At a sideslip angle of 0°, the drag coefficients for all dorsal fin variations were similar, showing a general increase in drag as the AoA increased, as expected from typical aerodynamic behavior. This trend follows the established principles of aerodynamics, where a higher AoA leads to increased airflow separation, and consequently, a higher drag.

As the sideslip angle increased to 5° and 10°, an interesting trend emerged: the drag values for all dorsal fin variations decreased slightly compared to the 0° sideslip condition, indicating an

improvement in the aerodynamic performance under non-zero sideslip conditions. Particularly notable is Variation 4, which demonstrates the lowest drag across all AoA and sideslip configurations, particularly at a 10° sideslip. This suggests that Variation 4 offers the best drag reduction, likely because of its optimal design, which minimizes flow separation and enhances the aerodynamic efficiency of the UAV under higher sideslip conditions. These findings emphasize the importance of the dorsal fin configuration in optimizing drag characteristics, particularly for UAVs operating under conditions with significant sideslip.

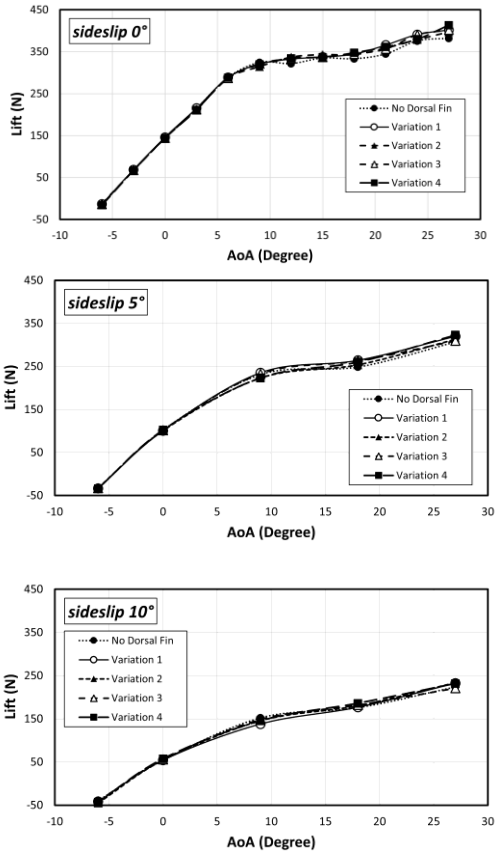

Figure 6 Graph of Lift versus AoA under the following conditions: *sideslip* 0°, *sideslip* 5°, and *sideslip* 10°.

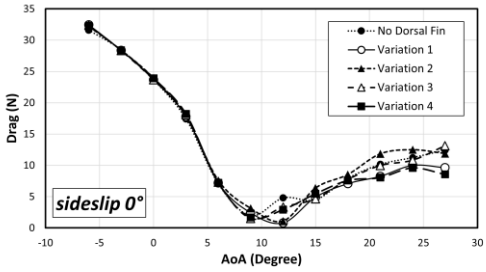

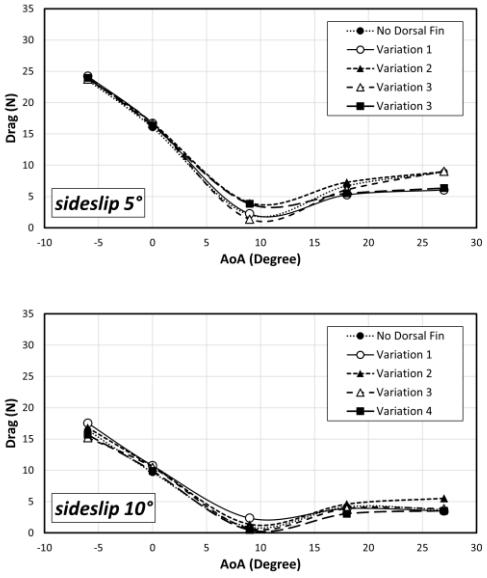

Figure 7 Graph of Drag versus AoA under the following conditions: *sideslip* 0°, *sideslip* 5°, and *sideslip* 10°

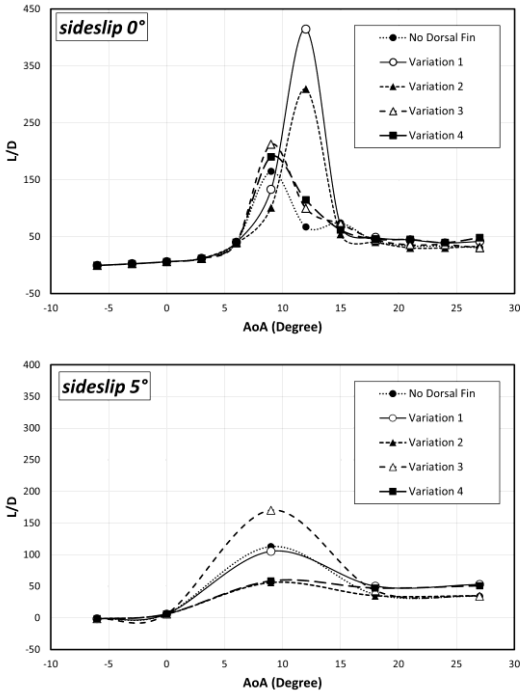

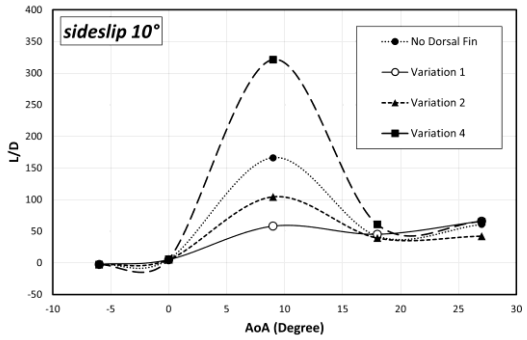

Figure 8 Graph of L/D vs. AoA under the following conditions: *sideslip* 0°, *sideslip* 5°, and *sideslip* 10°

The lift-to-drag ratio (L/D) is a key indicator of aerodynamic efficiency because it represents the ability to generate lift while minimizing drag. A higher L/D ratio is desirable for sustained flight efficiency because it enables a UAV to maintain lift with minimal drag. For a sideslip angle of 0°, Variation 1 exhibited the highest L/D ratio, suggesting that it had the best aerodynamic efficiency, particularly at a lower AoA. This trend is expected because higher C_L values coupled with moderate drag result in an optimal L/D ratio at low AoA.

However, as the AoA increased and the UAV transitioned to higher-drag regimes, the L/D ratio decreased across all variations, reflecting the increased drag associated with a higher AoA. In this context, the L/D ratio for all variations decreased, as expected, because of the inherent aerodynamic losses associated with a higher AoA. Nevertheless, when the sideslip increased to 5° and 10°, the L/D ratio improved slightly for all variations, with Variation 4 performing best at a 10° sideslip. This suggests that Variation 4 offers the best overall aerodynamic efficiency under higher sideslip conditions, likely because of its ability to balance the effects of lift and drag, while minimizing the negative impact of lateral wind components on performance.

The coefficient of yawing moment (C_N) is a critical measure of the directional stability of a UAV, as it quantifies the yawing moment generated during flight, which is influenced by sideslip and AoA. At a sideslip angle of 0°, the C_N increased steadily with the AoA, exhibiting a nearly linear trend for all dorsal fin variations. This indicates that, as the AoA increases, the UAV experiences more yaw, which can lead to stability issues.

When the sideslip angle was increased to 5° and 10°, the presence of dorsal fins became more significant in reducing the yaw moment. In particular. Variation 2 showed the most promising results in reducing yaw at a 5° sideslip, suggesting that the dorsal fin design in this variation effectively mitigated the yawing instability under these conditions. At a 10° sideslip, Variation 4 consistently provided better stability, demonstrating the increased effectiveness of the dorsal fins in enhancing directional stability at higher sideslip angles. These results highlight the role of dorsal fins in improving the ability of UAVs to maintain directional stability, particularly under conditions involving significant yaw and lateral-wind components.

The aerodynamic effects of adding a dorsal fin were analyzed using Computational Fluid Dynamics (CFD) simulations, with a focus on lift, drag, and yaw moments derived from pressure contours and streamlines around the UAV. The pressure contours indicate that the pressure beneath the UAV was higher than that on its upper surface, indicating the generation of lift. As the angle of attack (AoA) increased, the lift also increased, accompanied by a higher drag, which reduced propulsion efficiency. Larger AoAs lead to airflow separation over the wings, potentially causing stall, a condition in which lift is lost at critical AoAs. Streamlines at low AoAs demonstrated a stable flow, whereas flow separation was observed at high AoAs.

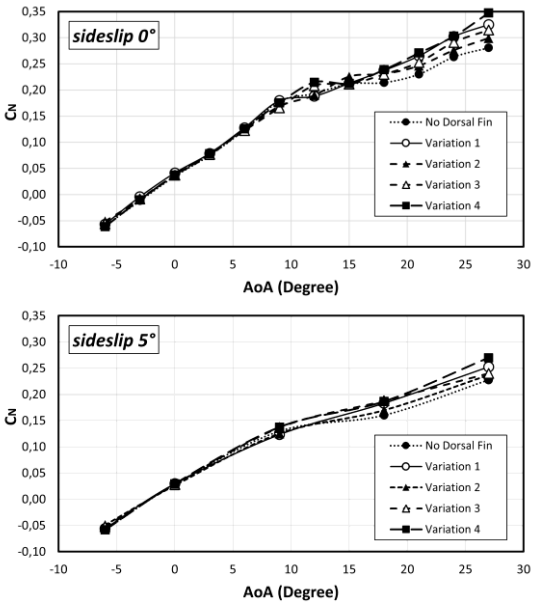

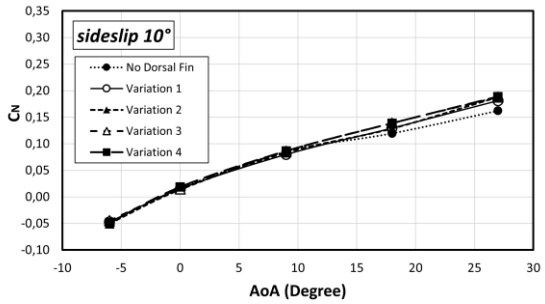

Figure 9 Graph of C_N vs. AoA under the following conditions: *sideslip* 0°, *sideslip* 5°, and *sideslip* 10°

CONCLUSION

Aerodynamic Performance at Optimal Angles of Attack (AoA). The simulation results demonstrated that the maximum lift-to-drag ratio was achieved at angles of attack (AoAs) between 9° and 12° when utilizing Variation 1 of the dorsal fin with with the smallest dorsal fin height 0,218 m. This variation significantly enhances the aerodynamic efficiency of the UAV, producing a substantial lift force while minimizing the drag. This indicates that variation 1 is particularly effective in optimizing the overall aerodynamic performance of the UAV, contributing to better fuel efficiency and improved flight performance.

Impact of Sideslip Angle on UAV Stability. As the sideslip angle increased, the simulation revealed a corresponding decrease in key aerodynamic parameters, including the lift coefficient, drag coefficient, lift-to-drag ratio, and yaw moment. This suggests that UAV stability is adversely affected as the sideslip increases. Additionally, the dorsal fin configuration minimally influenced these parameters when the sideslip angle was 0° or at low AoA. This indicates that under these specific conditions, the dorsal fin does not substantially affect UAV performance.

ACKNOWLEDGMENT

The authors would like to express their gratitude to all the parties who supported the completion of this research, especially Kelvin Kurniawan and Hendra Faisal, as assistant researchers. This research was funded by the Faculty of Engineering, Gadjah Mada University (Grant No. 1610402/UN1). FTK/SK/HK/2025).

REFERENCES

[1] Y. A. Abd Rahman, M. T. Hajibeigy, A. S. M. Al-Obaidi, and K. H. Cheah, "Design and Fabrication of Small Vertical-Take-Off-Landing Unmanned Aerial Vehicle," *MATEC Web Conf.*, vol. 152, p. 02023, 2018, doi: 10.1051/matecconf/201815202023.

[2] A. Mukherjee, S. Misra, and N. S. Raghuwanshi, "A survey of unmanned aerial sensing solutions in precision agriculture," *Journal of Network and Computer Applications*, vol. 148, p. 102461, Dec. 2019, doi: 10.1016/j.jnca.2019.102461.

[3] P. Radoglou-Grammatikis, P. Sarigiannidis, T. Lagkas, and I. Moscholios, "A compilation of UAV applications for precision agriculture," *Computer Networks*, vol. 172, p. 107148, May 2020, doi: 10.1016/j.comnet.2020.107148.

[4] B. Allred, N. Eash, R. Freeland, L. Martinez, and D. Wishart, "Effective and efficient agricultural drainage pipe mapping with UAS thermal infrared imagery: A case study," *Agricultural Water Management*, vol. 197, pp. 132–137, Jan. 2018, doi: 10.1016/j.agwat.2017.11.011.

[5] E. R. Hunt, M. Cavigelli, C. S. T. Daughtry, J. E. Mcmurtrey, and C. L. Walthall, "Evaluation of Digital Photography from Model Aircraft for Remote Sensing of Crop Biomass and Nitrogen Status," *Precision Agric*, vol. 6, no. 4, pp. 359–378, Aug. 2005, doi: 10.1007/s11119-005-2324-5.

[6] D. Scholz, "Empennage sizing with the tail volume complemented with a method for dorsal fin layout," *INCAS BULLETIN*, vol. 13, no. 3, pp. 149–164, Sept. 2021, doi: 10.13111/2066-8201.2021.13.3.13.

[7] G. Nugroho, G. Zuliardiansyah, and A. A. Rasyiddin, "Performance Analysis of Empennage Configurations on a Surveillance and Monitoring Mission of a VTOL-Plane UAV Using a Computational Fluid Dynamics Simulation," *Aerospace*, vol. 9, no. 4, p. 208, Apr. 2022, doi: 10.3390/aerospace9040208.

[8] F. Nicolosi, D. Ciliberti, and P. Della Vecchia, "Aerodynamic Design Guidelines of Aircraft Dorsal Fin," in *34th AIAA Applied Aerodynamics Conference*, Washington, D.C.:

American Institute of Aeronautics and Astronautics, June 2016. doi: 10.2514/6.2016-4330.

[9] Y. Ito, M. Murayama, S. Koike, K. Yamamoto, K. Nakakita, and K. Kusunose, "Computational Investigation of Vertical Stabilizer with Vortex Generators and Dorsal Fin," *Journal of Aircraft*, vol. 56, no. 5, pp. 1833–1848, Sept. 2019, doi: 10.2514/1.C035301.

[10] S. Gudmundsson, "The Anatomy of the Tail," in *General Aviation Aircraft Design*, Elsevier, 2014, pp. 459–519. doi: 10.1016/B978-0-12-397308-5.00011-8.

[11] B. Dai, Y. He, F. Gu, L. Yang, J. Han, and W. Xu, "A vision-based autonomous aerial spray system for precision agriculture," in *2017 IEEE International Conference on Robotics and Biomimetics (ROBIO)*, Macau: IEEE, Dec. 2017, pp. 507–513. doi: 10.1109/ROBIO.2017.8324467.

[12] P. Skobelev, D. Budaev, N. Gusev, and G. Voschuk, "Designing Multi-agent Swarm of UAV for Precise Agriculture," in *Highlights of Practical Applications of Agents, Multi-Agent Systems, and Complexity: The PAAMS Collection*, vol. 887, J. Bajo, J. M. Corchado, E. M. Navarro Martínez, E. Osaba Icedo, P. Mathieu, P. Hoffa-Dąbrowska, E. Del Val, S. Giroux, A. J. M. Castro, N. Sánchez-Pi, V. Julián, R. A. Silveira, A. Fernández, R. Unland, and R. Fuentes-Fernández, Eds., in Communications in Computer and Information Science, vol. 887. , Cham: Springer International Publishing, 2018, pp. 47–59. doi: 10.1007/978-3-319-94779-2_5.

[13] C. A. Rokhmana, "The Potential of UAV-based Remote Sensing for Supporting Precision Agriculture in Indonesia," *Procedia Environmental Sciences*, vol. 24, pp. 245–253, 2015, doi: 10.1016/j.proenv.2015.03.032.